Synthesize and Fabrication of Supramolecular Polydimethylsiloxane based Nanocomposite Elastomer for Versatile and Intelligent Sensing

Xin Jing[a], *Zhenping Ma*[a], *Maxwell Fordjour Antwi-Afari*[d], *Lin Wang*[b], *Heng Li*[c], *Hao-Yang Mi*[*,a,b], *Pei-Yong Feng*[*,a], *Yuejun Liu*[a]

[a] Key Laboratory of Advanced Packaging Materials and Technology of Hunan Province, Hunan University of Technology, Zhuzhou, 412007, China.

[b] National Engineering Research Center for Advanced Polymer Processing Technology, Zhengzhou University, Zhengzhou, 450000, China.

[c] Department of Building and Real Estate, Hong Kong Polytechnic University, Hong Kong, 518000, China.

[d] Department of Civil Engineering, College of Engineering and Physical Sciences, Aston University, Birmingham, B4 7ET, United Kingdom.

Corresponding authors:

H.Y. Mi E-mail: mihaoyang@zzu.edu.cn

P.Y. Feng E-mail: fpyedu@163.com

ABSTRACT

High-performance strain sensors featured with self-healing ability and high stretchability are desired for human motion detection, soft robotics, and diver intelligent applications. Herein, a novel self-healing elastomer was synthesized via a facile one-pot polycondensation reaction between bis(3-aminopropyl) terminated polydimethylsiloxane (PDMS) and 2,4'-tolylene diisocyanate (TDI), followed by introducing carboxyl-functionalized multi-walled carbon nanotubes (CNT). The physically entangled linear molecular chains and multiple hydrogen bonds endowed elastomer with a remarkable healing efficiency of 98.1 % and outstanding stretchability of over 1000 %. Attributing to the conductive network constructed by the uniformly dispersed CNT, the nanocomposite elastomer-based strain sensor achieved a high gauge factor of 2.43 and its sensing performance could be well regained after self-healing. The strain sensor was successfully used for detecting various human motions, and distinguishing facial micro-expressions. Moreover, the nanocomposite elastomer applied on a grip ball and woolen glove as sensing units rendered them with the ability of grip force detection and sign language recognition. This work offers a new route and a promising self-healing nanocomposite elastomer for the development of recyclable and sustainable high-performance strain sensors, and prospects its advanced intelligent applications.

Keywords: Self-healing polymer; Elastomer; Nanocomposite; Strain sensor; Carbon nanotubes

1. INTRODUCTION

Human motion and health monitoring are becoming a rising cutting-edge field for improving the wellness of human being.[1, 2] Novel wearable and flexible sensors are originated from the idea of mimicking the function of human skin which can measure diverse signals such as strain, pressure, humidity, and temperature by transducing biological or mechanical signals into electrical signals.[3-5] To satisfy the increasing demand for advanced intelligent applications, such as human motion detection,[6] patient behavior monitoring,[7] human-computer interaction,[8] and sign language identification,[9-11] flexible strain sensors have been heavily investigated in recent years. Developing sustainable, stable, and recyclable strain sensors that can be easily integrated with existing medical devices, clothes, electronics, and among others are the pursuits of the field.[12]

Resistive-type strain sensor is a type of widely used sensor because it has advantages of being transformed into variety of forms, low cost, and simple structure.[13, 14] They are typically fabricated by assembling conductive sensing networks on the surface of polymeric substrates and within the polymer matrix.[15] However, many problems exist in flexible strain sensors, e.g., the cracks on the conductive layer would cause performance deterioration in long-term and low stability; the nonuniform dispersion of conductive fillers may lead to low sensitivity; and majority strain sensors suffer from limited sensing strain range due to the low stretchability of the substrate material.[16, 17] Thus, improving the stretchability, stability, and applicability are of significance for the development of sustainable high-performance strain sensors.[18-21]

Self-healing polymeric materials provide new thoughts for sustainable strain sensors,[22-24] since they could trigger spontaneous or stimulated self-healing process because of the reversible associations, e.g., hydrogen bonds,[25] Diels-Alder bonds,[26] disulfide bonds,[27] and metal-ligand coordination bonds,[28] etc, presented in their molecular chains, so that they are

also classified as supramolecule materials. During the past few years, extensive efforts have been made to develop self-healing materials including highly stretchable elastomers. For example, Raimondo et al.[29] prepared a self-healing PDMS/CNT nano-hybrid using 4,4'–diaminodiphenyl sulfone functionalized CNT and benzoxazine terminated PDMS. This work provided an effective method of covalent and non-covalent functionalizations to enhance the interactions of CNT with elastomer matrix. In addition, Zheng et al.[30] reported a multi stimuli-responsive self-healing polyurethane (PU) elastomer by in situ polymerizations of hydroxyl-functionalized CNT and PU matrix, then metallo-supramolecular PU/CNT nanocomposite was obtained after crosslinking with Zn^{2+}, which exhibited self-healing ability. These advanced achievements offer a good idea of synthesizing self-healing elastomers.

Regarding the application of strain sensing, various flexible and stretchable polymeric composites have been proposed aiming to enhance the sensitivity, response time, sensing range, etc. Indeed, elastomers have been utilized as flexible substrates for flexible strain sensors by combining with conductive fillers including CNT,[31] graphene,[32] Mxenes,[33] metallic nanowires,[34] and metallic nanoparticles.[35] PU elastomer possess promising flexibility, stretchability, and human skin affinity that have been recognized as ideal substrates for flexible strain sensors. However, the highly crosslinked chemical structure of PUs make them difficult to be recycled and applied in autonomous circumstances.[36] Moreover, the efforts made on high-performance strain sensors that have self-healing property and high stretchability are rare.

In this study, by combining the advantages of PDMS and PU, we developed a PDMS based PU elastomer with a linear molecular chain and rich multiple hydrogel bonds as a self-healing elastomeric matrix. The elastomer was synthesized via a simple one-pot polycondensation reaction between aminopropyl terminated PDMS and TDI at mild conditions, and carboxyl-functionalized CNT (CNT-COOH) was introduced into the PDMS-

TDI elastomer matrix by solution mixing. The CNT-COOH not only created a conductive network in the elastomer matrix, but also enriched the hydrogen bonds with the nanocomposite, which contributed to the high stretchability, self-healing ability, and sensitivity of the elastomer. The as-prepared strain sensor based on the nanocomposite elastomer demonstrated excellent performance in detecting human motion, facial-micro expression, and handwriting. The thermoplastic property of the nanocomposite elastomer made it capable to be applied in diverse applications. A smart glove featured with the strain sensors could recognize sign language changes by detecting movements of different finger joints.

2. EXPERIMENTAL

2.1 Materials

Aminopropyl terminated polydimethylsioxane (H_2N-PDMS-NH_2, abbreviated as PDMS, Mn=5000) was purchased from Meryer (Shanghai) Chemical Technology Co., Ltd., China. 2,4'-tolylene diisocyanate (TDI) and methanol (MeOH) were purchased from Shanghai Macklin Biochemical Co., Ltd. Triethylamine (Et3N) and carboxyl-functionalized multi-walled CNTs (CNT-COOH, inner diameter: 5-10 nm; outer diameter: 10-20 nm; length: 0.5-2 μm) were purchased from Aladdin Reagent Co., Ltd., China. Tetrahydrofuran (THF) was obtained from Sinopharm Chemical Reagent Co., Ltd. Anhydrous chloroform (TCM) was obtained from Tianjin Fuyu Chemical Co., Ltd. China. All chemicals were used as received without further purification.

2.2 Synthesis of PDMS-TDI elastomer

The PDMS-TDI elastomer was synthesized via a one-pot polycondensation reaction between PDMS and TDI. Briefly, 10.2 mL PDMS (2 mmol) and 0.5 mL Et3N were mixed with 10 mL TCM in a three-neck round bottom flask, and cooled to 0 ℃ in an ice bath and stirred for 1 h under argon atmosphere. A solution of 0.43 g TDI (2.5 mmol) dissolved in 2

mL TCM was added to the flask dropwise and mechanically stirred at 80 rpm for 1 h. Then, the temperature was raised to room temperature and stirred for another 3 h. After reaction, the transparent PDMS-TDI solution was poured slowly to 50 mL MeOH with stirring, and further stirred overnight. Finally, the PDMS-TDI elastomer was precipitated from MeOH and dried in a vacuum oven at 60 ℃ for 12 h.

2.3 Preparation of PDMS-TDI-CNT nanocomposites

Carboxyl-functionalized multi-walled CNTs were dispersed in THF by sonication for 1 h using a probe ultrasonicator (JY92-IIDN). A PDMS-TDI solution with 10 wt% concentration in THF was prepared by magnetic stirring at 25 ℃ for 1 h. To the PDMS-TDI solution, the as-prepared CNT dispersion was added quickly with vigorous magnetic stirring at 510 rpm for 4 h at 35 ℃. Then the mixture solution was poured into a polytetrafluoroethylene (PTFE) mold followed by degassing and drying using a vacuum oven at 60 ℃ for 12 h. The content of CNT was defined as the weight percentage of the PDMS-TDI elastomer matrix, which was controlled to be 1 wt%, 2 wt%, 3 wt%, 4 wt%, 5 wt%, and 6 wt% of the PDMS-TDI. The resulted composite films were coded as PDMS-TDI-xwt%CNT, where x stands for the concentration of CNT in the nanocomposite.

2.4 Fabrication of PDMS-TDI-CNT nanocomposite based sensors

A PDMS-TDI-CNT elastomer film with a size of 30 mm × 10 mm × 0.3 mm was prepared and sandwiched by two stripes of VHB tape as illustrated in Figure S1. Two copper wires were connected to the two ends of the elastomer as current leads to a multimeter to record the change resistance of the elastomer when it was deformed.

2.5 Characterizations

Field emission scanning electron microscopy (SEM, Zeiss Sigma 300) was used to observe the dispersion of CNT in PDMS-TDI elastomer. Samples were frozen in liquid nitrogen, fractured in the cross-section, and coated with a thin film of gold before imaging.

The chemical structure of synthesized PDMS-TDI elastomer was characterized using proton nuclear magnetic resonance spectroscopy (^{1}H NMR, Bruker 400M) with chloroform-d as solvent. The molecular weight and polymer dispersity index (PDI) of prepared PDMS-TDI elastomer was measured using a Waters 1525 & Agilent PL-GPC220 gel permeation chromatography (GPC) instrument with THF as the elution solvent at a flow rate of 0.67 mL/min. Fourier transform infrared (FT-IR) spectroscopy (Bruker Tensor 20) was used to characterize the chemical structure of PDMS-TDI elastomer and PDMS-TDI-CNT nanocomposites in the range of 4000–600 cm^{-1}. The thermal property was evaluated on a differential scanning calorimetry (DSC) instrument (TA Q2000). The samples were heated to 180 ℃ from room temperature, followed by cooling to -80 ℃ and re-heating to 180 ℃ at a heating and cooling rate of 5 ℃/min under nitrogen flow. The tensile test experiments were carried out on a SAAS EUT2503 universal mechanical testing instrument at room temperature at a strain rate of 10 mm/min.

The self-healing behavior was evaluated by observing the evolution of cracks using a depth-of-field optical microscope (DVM6, Leica, Germany). Optical images and z-stack height profile images were recorded during the self-healing process. The healing efficiency, which is defined as the ratio of stress strength of the healed sample to that of the original one as expressed in Equation (1),[25] was evaluated using the same mechanical tester.

$$\text{Healing efficiency (\%)} = \frac{\text{Healed tensile strength}}{\text{Original tensile strength}} \times 100\% \quad (1)$$

2.6 Characterization of PDMS-TDI-CNT nanocomposite based sensors

The relative change of resistance ($\Delta R/R_0$) of all fabricated flexible strain sensors was tested using BK Precision-878B two-electrode system when the sensors are subjected to deformation. In general, the resistance of the strain sensors is sensitive to strain and the $\Delta R/R_0$ was defined as Equation (2):[37, 38]

$$\Delta R/R_0 = \left(R - R_0\right)/R_0 \quad (2)$$

where R_0 was the initial resistance of the strain sensor when no tension was applied, $\Delta R=R-R_0$ and $\Delta R/R_0$ represented the value of resistance change and with a certain strain applied on the sensor, respectively.

The flexible strain sensors were attached to different joints of human body and monitor the motion of those joints by recording the change of resistance.

An electrochemical workstation (CHI 760e) was used to measure the real-time current signal of the strain sensors. The *i-t* curve of sensors upon deformation and recovery was recorded at a constant voltage of 10 V.

3. RESULTS AND DISCUSSION

3.1 Chemical and Morphological Properties of Self-Healing PDMS-TDI Elastomers

The self-healing PDMS-TDI elastomers were synthesized via a one-pot polycondensation reaction (Figure 1a). The terminating amino (–NH_2) groups of NH_2-PDMS-NH_2 were reacted with the –NCO groups of TDI with the presence of Et3N as catalyst forming a transparent PDMS-TDI gel. The unreacted –NCO groups and catalyst were neutralized and removed by MeOH soaking, and the PDMS-TDI elastomer incorporated with urea bonds was obtained through a facile one-step polymerization approach (Figure 1b). Here, NH_2-PDMS-NH_2 was selected to endow the elastomer with flexibility, which was beneficial for enhancing the comforts of wearable devices. The urea bonds could form strong intermolecular hydrogen bonds, which would not only act as physical crosslinking points to provide the elastomer with excellent stretchability, but also render the elastomer with a rapid self-healing attribute[39]. The weak hydrogen bonds between –NH and C=O of urea bonds are supposed to be able to dissipate strain energy and endow the elastomer with high stretchability. The synthesized PDMS-TDI elastomer is highly transparent and can be easily

dissolved in THF at room temperature attributing to the amorphous characteristic of the elastomer, which makes it easy to be recycled and reused (Figure S2).[40] The effect of the molecular weights of the PDMS prepolymer was investigated. The molecular weight results (Table S1) measured using GPC showed that the M_w of PDMS-TDI elastomer was increased with the increase of the molecular weight of the prepolymer. When the PDMS with a number average molecular weight of 5000 was used, the highest M_w of 3.95×10^4 g/mol and the lowest polymer dispersity index (PDI) of 1.99 were obtained, indicating that the synthesizd PDMS-TDI elastomer had a narrow molecular weight distribution and a uniform molecular weight.[25]

To further enhance the hydrogen bonds and create a conductive network in the PDMS-TDI elastomer so as to extend its application as flexible strain sensors, carboxyl-functionalized multi-walled CNTs were incorporated with the elastomer by simple ultrasound sonication assisted solution mixing and casting method (Figure 1c). The CNTs loading content in the PDMS-TDI-CNT nanocomposite elastomers was controlled at 1 wt%-6 wt%. As shown in the SEM images (Figure 1d-i), the CNTs were uniformly distributed in the PDMS-TDI matrix even at 6 wt% concentration. From the high magnification images, CNT agglomeration was not observed on all samples, and the CNTs were tightly bonded with the PDMS-TDI matrix, which suggested the excellent dispersibility of CNT in PDMS-TDI/THF solution, and the high compatibility between the CNT and the PDMS-TDI. Similar to the PDMS-TDI elastomer, the prepared PDMS-TDI-CNT nanocomposites maintained high flexibility and stretchability (Figure S3).

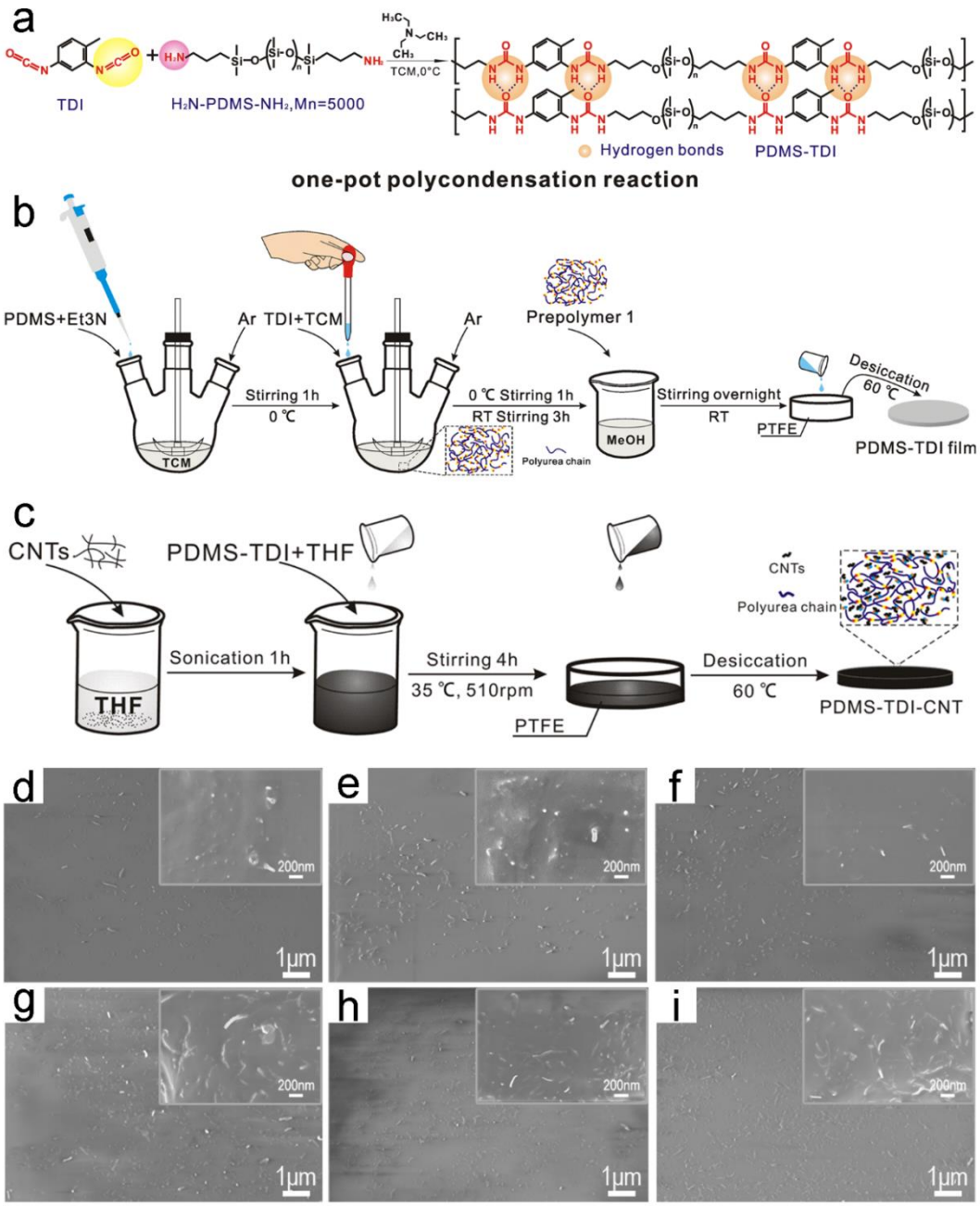

Figure 1. (a) Reaction mechanism of the synthesis of self-healing PDMS-TDI elastomer; (b) Schematic of one-pot polycondensation reaction and preparation of PDMS-TDI elastomer; (c) Preparation of PDMS-TDI-CNT nanocomposite elastomer; SEM images of PDMS-TDI-CNT nanocomposites with CNT concentration of (d) 1 wt%, (e) 2 wt%, (f) 3 wt%, (g) 4 wt%, (h) 5 wt%, and (i) 6 wt%.

The chemical structure of the synthesized PDMS-TDI elastomer was analyzed using ^{1}H NMR. As shown in Figure 2a, the peaks at 5.51 ppm and 6.05 ppm were assigned to the two

secondary amines of urea bonds,[39, 41] which indicated the existence of urea bonds and hydrogen bonds. Signal of the protons from PDMS chain are observed at -0.05 ppm,[42] the peak at 1.2 ppm and 3.70 ppm are associated to the methyl group from TDI.[42, 43] ^{1}H NMR demonstrated the successful synthesis of bulk PDMS-TDI, as indicated by the presence of characteristic peaks of TDI and PDMS segments in polymeric backbones. FT-IR was used to further analyze the chemical bonds of PDMS-TDI elastomer and PDMS-TDI-CNT nanocomposites (Figure 2b). The peaks at 1645 cm^{-1} and 1260 cm^{-1} correspond to the C=O and C–O bonds, suggesting the presence of urea bonds and further verified the successful synthesis of PDMS based polyurethane-urea.[41, 42, 44] The peaks located at 867 cm^{-1} and 1006 cm^{-1} were assigned to the absorption of Si–O of NH_2-PDMS-NH_2.[45] The absence of peaks at 2260 cm^{-1} ascribing to –NCO groups suggested that diisocyanate groups have been expended or removed through the reaction and purification.[46] The enhancement of characteristic peak of C–O (carboxy) at 1260 cm^{-1} as the increase of CNT concentration indicates the introductions of oxygen-containing functional groups from the CNT-COOH.[47] Upon introduction of CNTs, wide peaks appeared at 3200-3500 cm^{-1} can be assigned to the absorptions of –COOH.

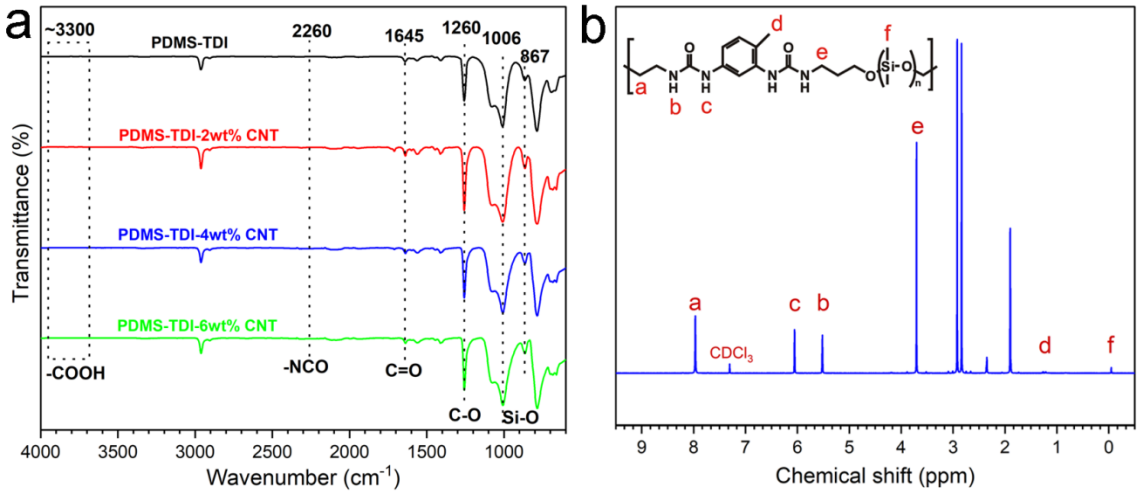

Figure 2. (a) FT-IR spectra of PDMS-TDI and different PDMS-TDI-CNT elastomers; (b) ^{1}H NMR spectrum of PDMS-TDI elastomer using chloroform-d as a solvent.

3.2 Self-healing and Mechanical Performance

The self-healing property is particularly desirable for multi-functional polymeric materials because it can make materials more reliable, reduce repair costs, and extend the service life of the materials or products.[30, 48, 49] The self-healing behavior of PDMS-TDI-4wt%CNT nanocomposite was observed using a depth-of-field optical microscope after cutting the sample using a razor blade. The samples were placed in an oven set at 60 ℃ to allow the recovery of the nanocomposite elastomer, and the cut section was imaged during the self-healing process. As shown in Figures 3a-c and d-f, the initial crevice of the cut PDMS-TDI-CNT film has a size of ~90 μm and a depth of 85 μm, and the crevice was gradually contracted when the film was thermally treated for up to 10 h. After 5 h of thermal treatment, the crevice size and depth were reduced to 12 μm and 25 μm, respectively, and the crevice was completely disappeared after 10 h suggesting the complete healing of the nanocomposite elastomer. The self-healing attribute of the PDMS-TDI-CNT nanocomposite was originated from the reconstruction of the hydrogen bonds and the diffusion of polymer chains at high temperature since the synthesized PDMS-TDI elastomer and the PDMS-TDI-CNT nanocomposites are amorphous with a glass transition temperature (T_g) of ~0 ℃ (Figure S4) which insured the thermal motion ability of the macromolecules.[50] Figure 3g illustrates the self-healing mechanism of the developed PDMS-TDI-CNT nanocomposites. The presence of multiple hydrogen bonds confer the PDMS-TDI-CNT nanocomposites autonomous self-healing capability, and the reconstruction of reversible hydrogen bonds could be effectively promoted under elevated temperature.[47]

The mechanical properties of PDMS-TDI elastomers with different molecular weights were investigated. It was found that the elastomer with the highest molecular weight exhibited the highest tensile strength and elongation at break, which were 30.9 kPa and 1275.4 %, respectively (Figure S5). This implies that superior mechanical property could be

obtained at high molecular weight due to the substantial chain entanglements. Considering the requirement of the strain sensor for tensile strength, we mainly focused on the sensing performance and self-healing property of with highest molecular weight. To quantitively characterize the healing efficiency of the synthesized elastomer and nanocomposites, samples (30 mm × 10 mm × 0.3 mm) were cut in the middle section by a razor blade in the direction perpendicular to the tensile direction (Figure S6). The self-healed PDMS-TDI elastomer could be stretched to 760 % strain after healing at 60 ℃ for 9 h as shown in Figure S7. The PDMS-TDI-CNT nanocomposite could restore its original stretchability after being healed at 60 ℃ for 9 h. As shown in Figure S8 and Movie S1, the healed PDMS-TDI-4wt%CNT exhibited similar stretchability with the pristine composite, and could be easily stretched to over 900 % strain. The tensile strength was measured before and after the self-healing process to assess the self-healing efficiency. As expected, the tensile strength and tensile modulus were increased as the increase of CNT content in the PDMS-TDI-CNT nanocomposites (Figure S9), which was attributed to the synergetic effects of high stiffness of CNT, π-conjugated network, multiple hydrogen bonds formed in PDMS-TDI-CNT matrix, and the good dispersion of CNTs in the matrix.[51] The tensile stress of the PDMS-TDI film was 31.5 kPa, and it was dramatically improved to 110.2 kPa for the PDMS-TDI-6wt%CNT film, while the strain-at-break maintained around 1200 % for all PDMS-TDI-CNT nanocomposite films (Figure S10), since the supramolecular network can effectively dissipate strain energy through the rupture of weak hydrogen bonds, while the strong covalent bonds would be sufficient to maintain the high tensile stress.[43] Figure 3h and 3i show the tensile strength and the healing efficiency of PDMS-TDI, PDMS-TDI-3wt%CNT, and PDMS-TDI-6wt%CNT after self-healing for 6 h and 9 h at 60 ℃. The hydrogen bonds were increased with the increase of CNT content in the elastomer attribute to the healing efficiency was heightened. The healing efficiency of PDMS-TDI was 83.8 % after 9 h, while the PDMS-

TDI-3wt%CNT and PDMS-TDI-6wt%CNT samples achieved a remarkable healing efficiency of 98.1 %, which surpasses majority self-healing polymers or hydrogels developed recently (Table S2). Moreover, the self-healed PDMS-TDI-3wt%CNT nanocomposite regain about the same tensile behavior as the original sample after 9 h of healing (Figure S11). The significant self-healing performance improvement of the PDMS-TDI-CNT nanocomposite was because of the multiple hydrogen bonds formed in PDMS-TDI-CNT matrix as well as the high flexibility of the molecular chains at elevated temperatures, which facilitated the thermal motion of molecular chains and reconstruction of the hydrogen bonds in the damaged area.[39, 52]

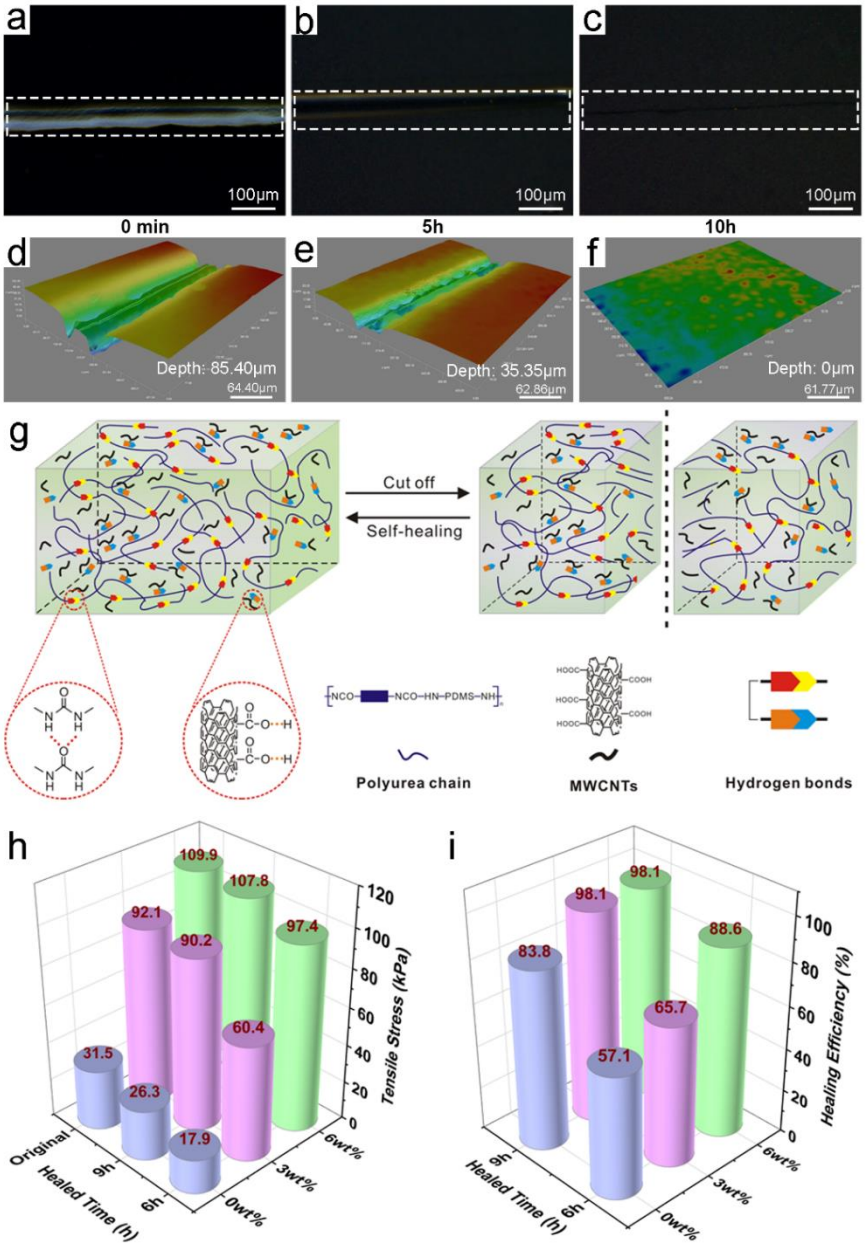

Figure 3. (a-c) Optical microscope images for the healing process of the PDMS-TDI-4wt%CNT nanocomposite film at 60 ℃ for up to 10 h. (d-f) corresponding depth-of-field images show the height mapping during the self-healing process. (g) Schematic illustration of the self-healing process of PDMS-TDI-CNT elastomer based on multiple hydrogen bonds. (h) Tensile strength and (i) healing efficiency of PDMS-TDI, PDMS-TDI-3wt%CNT, and PDMS-TDI-6wt%CNT films after healing at 60 ℃ for 6 h and 9 h.

3.3 Sensing Performance of the PDMS-TDI-CNT based Strain Sensor

For the application of flexible and wearable sensors, the sensing material should be mechanically durable, with a good frequency response and low electrical hysteresis under mechanical deformation.[53] The resistivity of different PDMS-TDI-CNT nanocomposites is shown in Figure 4a, from which it can be seen that the conductivity was improved significantly as the CNT content was increased from 1 wt% to 4 wt%, and the improvement became less significant when the CNT content was further increased to 6 wt%. Therefore, PDMS-TDI-4wt%CNT composite elastomer was selected as an example to investigate its sensing performance. Gauge factor (GF), which is determined by the change in the resistance at a certain strain $(\Delta R/R_0)/\varepsilon$ (ε is the applied strain), is an important factor related to the sensitivity of a strain sensor. Generally, a broad sensing range is preferred for large motion monitoring, while sensing minor strains caused by subtle motions such as facial expression requires high GF.[54] As shown in Figure 4b, the relative resistance changes increased almost linearly under the external strain, which might be attributed to the uniform deformation of the polymer network during the stretching process. Amazingly, the nanocomposite elastomer still showed a stable resistance, even when it had been stretched to 1000 % strain. In addition, the $\Delta R/R_0$ increases linearly in the first strain region (ε < 150 %) with a high gauge factor of 2.43, and then this value drops to 1.51 and 0.65 in the strain range from 150 % to 700 % and range from 700 % to 1000 %, respectively. The different sensing regions are attributed to the viscoelastic behavior of the elastic supporting substrate.[43] In practical application, it would be more precise to specify the GF in different sensing strain ranges.

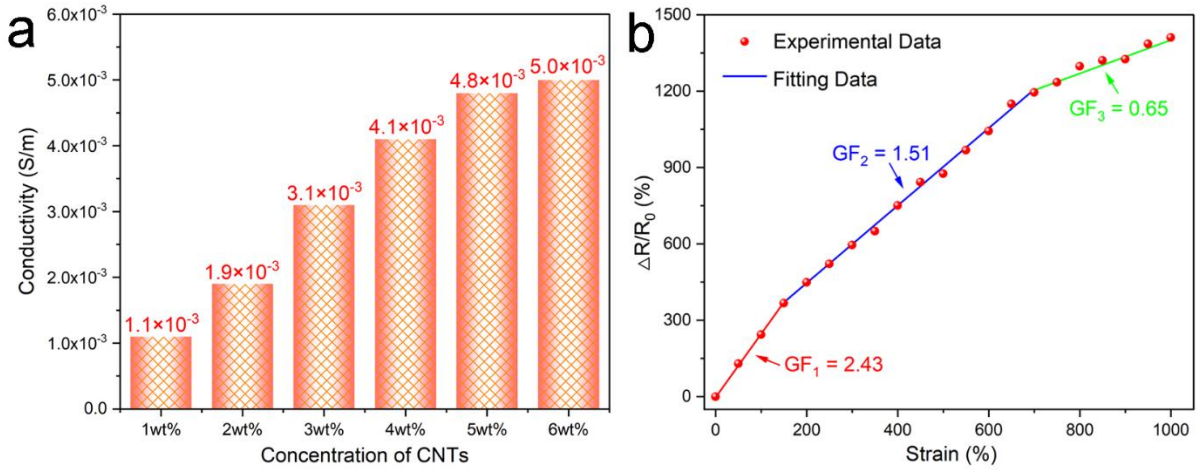

Figure 4. (a) Conductivity of different PDMS-TDI-CNT nanocomposite elastomers; (b) GF of PDMS-TDI-4wt%CNT nanocomposite in the strain range of 0-1000%.

Wearable strain sensors are often mounted on the skin to monitor body movement, particularly the movement of joints such as the finger, wrist, and elbow that can be affected by ageing, injury, and diseases.[55] The resistance of strain sensors is defined as Equation (3), and R and $\Delta R/R_0$ values would increase when the strain sensors are been stretched or deformed. The intensity of the signal is mainly determined by the magnitude of deformation.

$$R = \rho \frac{L}{S} \tag{3}$$

where ρ refers to the resistivity, L and S are the lengths and cross-section area of the conductor.

Figure 5a shows the recorded real-time change of resistance as the index finger was repeatedly bent and straightened with an angle up to 120 °. Figure 5b and c demonstrated the detection of repetitive wrist and elbow bending motion. Similarly, the resistance of the strain sensor increased during the bending, and returned to the original value when the wrist and elbow were recovered. The real-time current changes signals of wrist and knee joint bending were shown in Figure S12 which further confirmed the outstanding stability and fast response of the PDMS-TDI-CNT-based strain sensors. In addition to large-scale human motion surveillance, the strain sensor could be utilized to monitor and recognize facial micro-

expressions (e.g., frown, blink, and cheek-bulge). As shown in Figure 5d, the $\Delta R/R_0$ signal could well reflect the facial expression change from a relaxed state to cheek-bulging, and the signal curve showed quite good repetitive patterns with the repeated cheek-bulging. The strain sensor was attached to the tester's forehead to further detect the frowning motion on the forehead (Figure 5e). The stretching of muscles around the forehead during tester frowning caused the tension of the sensor,[56] which could be recorded by the change of $\Delta R/R_0$ signal. The repetition frowning motion resulted in a similar $\Delta R/R_0$ signal as shown in the real-time recording curve. Moreover, the strain sensor developed was also able to detect the motion of eye blinking as shown in Figure 5f. According to the equation (2) and (3), the lower $\Delta R/R_0$ was caused by the relatively small strain change when measuring the eye blinking. These results verified the feasibility of the PDMS-TDI-CNT nanocomposite elastomer-based strain sensor to serve as an emotion detector to monitor the emotional variation of human beings.

The developed strain sensor also showed excellent sensitivity to bending angles. When the bending angle was increased from 0 ° to 120 °, the $\Delta R/R_0$ increased accordingly (Figure 5g). The relationship between the bending angle and relative resistance changes can be fitted with a quartic function with a small a, b, and c factors, which implies a good linearity of the PDMS-TDI-CNT-based sensor when detecting the change of bending angle. The measurement of bending angle was evaluated by a simple finger bending experiment, As tested in Figure 5h, the $\Delta R/R_0$ signal was gradually increased as the bending angle was increased from 0 ° to 120 °. Meanwhile, the signal of the strain sensor maintained almost the same when repeating the finger bending at the same angle indicating high sustainability and stability. The regeneration of the sensing ability of the strain sensor was also investigated by cutting the PDMS-TDI-CNT film into two separate pieces and allow them to heal at 60 ℃ for 9 h. As shown in Figure 5i and Movie S2, the *i-t* curve indicated that the strain sensor could regain sensing capability after self-healing, and the current maintained in the same

level with the original sensor attributing to the regeneration of hydrogen bonds in the cut region and the reconstruction of CNT conductive network. Considering the critical movement strain of human motion to be about 50 %,[57] the stability and durability of as-prepared strain sensor was evaluated under the applied strain of 100 % and stretching speed of 100 mm min^{-1}. As displayed in Figure S13, it is obvious that the PDMS-TDI-CNT elastomer-based sensor exhibits a stable and reliable performance even after 1000 stretching-releasing cycles. Such excellent durability greatly assures the effective working of the sensor in the potential applications. All these results revealed the outstanding repeatability, durability, responsiveness, and excellent self-healing property of the PDMS-TDI-CNT elastomer-based strain sensor, and demonstrated its potential application in wearable devices for body motion and facial expression monitoring.

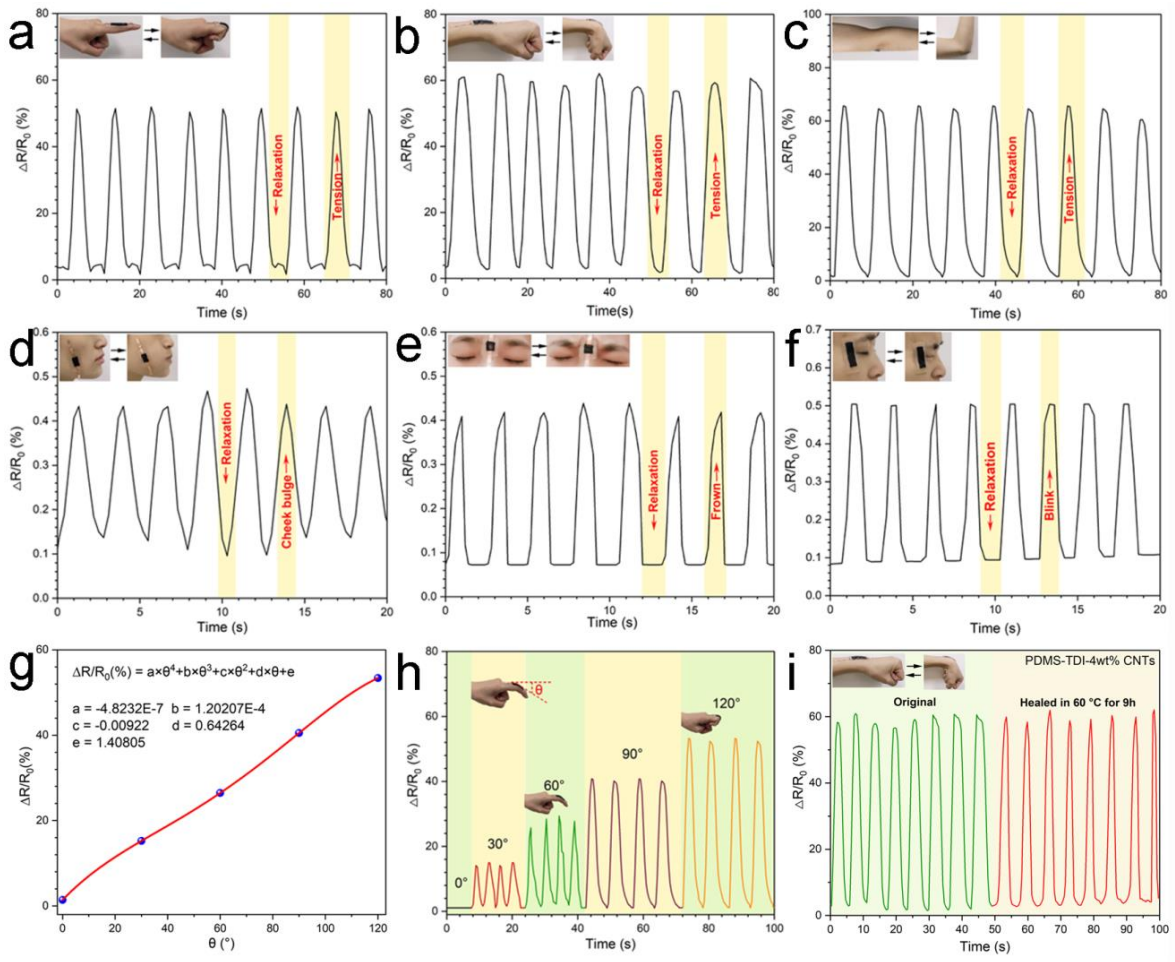

Figure 5. Sensing performance of the strain sensor based on PDMS-TDI-4wt%CNT elastomer for human motions and facial expression detection: (a) index finger joint bending, (b) wrist joint bending, (c) elbow joint bending, (d) cheek-bulging, (e) frowning, and (f) blinking. Inset photographs show the corresponding motions of the tester. (g) $\Delta R/R_0$ change in dependence on the bending angle from 0 ° to 120 ° and corresponding fitted curve; (h) $\Delta R/R_0$ signal of index finger bending to different angles monitored using the developed sensor; (i) Electric current signal of the strain sensor before and after self-healing at 60 ℃ for 9 h when detecting wrist joint bending.

3.4 Diverse Applications of the PDMS-TDI-CNT based sensor

In addition to human motion detection, the developed PDMS-TDI-CNT-based sensor could find diverse applications in intelligent sensing and human-computer interaction, and intelligent control. Attributing to the easy processability of the PDMS-TDI-CNT elastomer, it could be applied to various substrates as a conductive sensing coating unit. For example, five sensing units were coated on a grip ball and connected in series to feature the grip ball with sensing capability. Each unit corresponds to a finger pressing point, and the current intensity represents the pressing force on the grip ball. As shown in Figure 6a and Movie S3, the real-time current signal was higher, when the grip ball was pressed with more fingers, and each pressing cycle was indicated by a current peak. The corresponding peak current when the grip ball was pressed using different fingers could be fitted with a quartic function, and the a and b factors were one order of magnitude lower than the c and d factors, which suggested a moderate linearity in detecting finger pressure (Figure 6b). In addition, the PDMS-TDI-CNT-based sensor could serve as a piezoresistive pressure sensor to recognize the capital letters written on the surfaces of itself using a gel pen by means of the discrepancy in the number of strokes and the writing strength for different letters (Figure 6c). Moreover, the strain sensor was also utilized to recognize the other capital letters by means of the discrepancy in the

number of strokes. It was interesting to note from the real-time current signal that the signal of each letter showed a different characteristic and repeatable peak pattern, e.g., letters “E” and “M” have three and four strokes, respectively. And the current signal corresponds to arise three and four characteristic peaks, each peak corresponds to a stroke (Figure 6d). Due to the unique characteristic of letters “O” and “I” including writing direction and stroke, the elastomer-based sensor can yield one and two characteristic current signals to easily distinguish different letters written (Figure S14). Obviously, when the same letter was repeatedly written, the characteristic signals remain excellent repeatability and stability. Taking advantage of the unique recognition characteristics of handwriting habits, the elastomer-based sensor has great application prospects in intelligent writing and identity recognition.

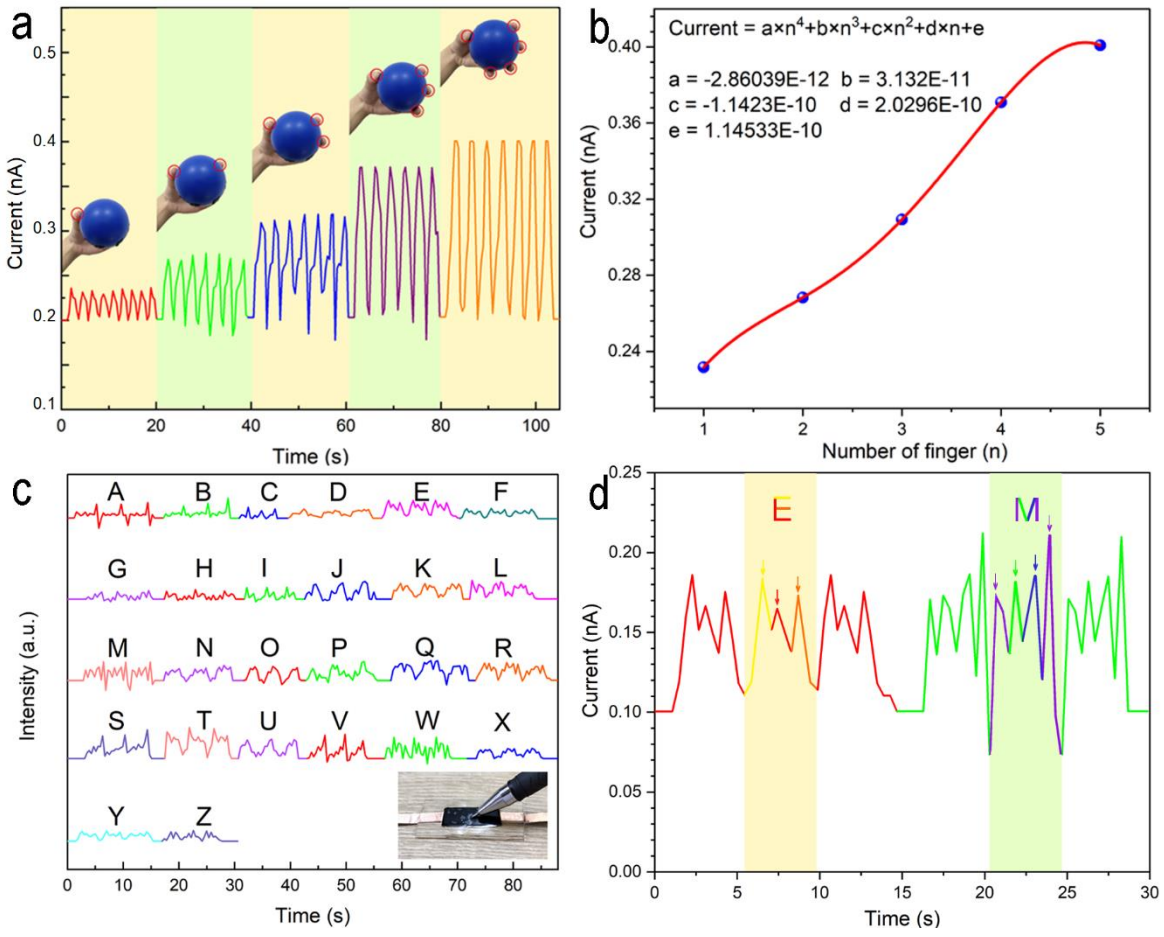

Figure 6. (a) Electric current signal of five sensor units attached on a grip ball when pressed using different numbers of fingers; (b) The fitting curve and quartic function relationship between the peak current and number of fingers; (c) Real-time current signal of the developed sensor using a gel pen writing on its surface for distinguishing 26 capital letters; (d) The piezoresistive response signal of "E" and "M" letters written on the elastomer-based sensor.

In addition, the PDMS-TDI-CNT nanocomposite could be coated on other flexible substrates to render them with sensing ability. Compared with conventional conductive past that is easy to crack and fail in repetitive usage,[58] the highly flexible self-healing PDMS-TDI-CNT nanocomposite coating would provide superior sustainability and reliability. As a demonstration, a thin layer of PDMS-TDI-CNT nanocomposite was coated on a rubber band, and the band was instantly featured with stain sensing ability with fast response and excellent stability (Figure S15).

Smart gloves incorporated with the PDMS-TDI-CNT sensing units were designed to fulfill the detecting and recognition of human sign language. To prepare the smart gloves, the viscous PDMS-TDI-CNT composite solution dissolved in THF was applied on the fingers of a fabric glove using a hairbrush followed by attaching of current leads and drying at 60 ℃ for 12 h. Figure 7a shows a smart glove with sensor units attached to the proximal interphalangeal joints to detect large deformation in finger movement, and Figure 7b illustrates a smart glove with sensor units attached to the metacarpophalangeal joints to monitor small deformation in finger movement. As shown in Figure 7c and Movie S4, the real-time current signal clearly revealed that the movement of each finger could be accurately detected by each sensor, and the signal peaks of thumb and litter finger were much weaker than the other three fingers since they have smaller deformation when bending. In the same manner, the smart glove could also recognize the gestures of fingers with small deformation. As shown in Figure 7d, when making sign language actions of "L, O, V, E", corresponding

current signals were generated on the fingers that have moved, which suggested that the bending strain of hand joints could be accommodated by the sensors. The fast and accurate response of the smart glove to hand movements manifests the high sensitivity of the developed PDMS-TDI-CNT-based sensor in real-time detection of micro-motions. Thus, the sign language could be read correctly by simply gathering the movement data obtained from the sensor units, which is highly favorable for distinguishing complex and similar human motions and holds great potential in advanced fields like gesture recognition, communication with deaf-mute people, human-computer interaction, and intelligent control.[59] Therefore, the developed PDMS-TDI-CNT nanocomposite could be comfortably integrated with fabrics and other flexible devices without significantly interfering with their properties, while featuring them with excellent sensing and recognition attributes that are highly desirable for human wellness enhancement and next generation wearable electronics.[60]

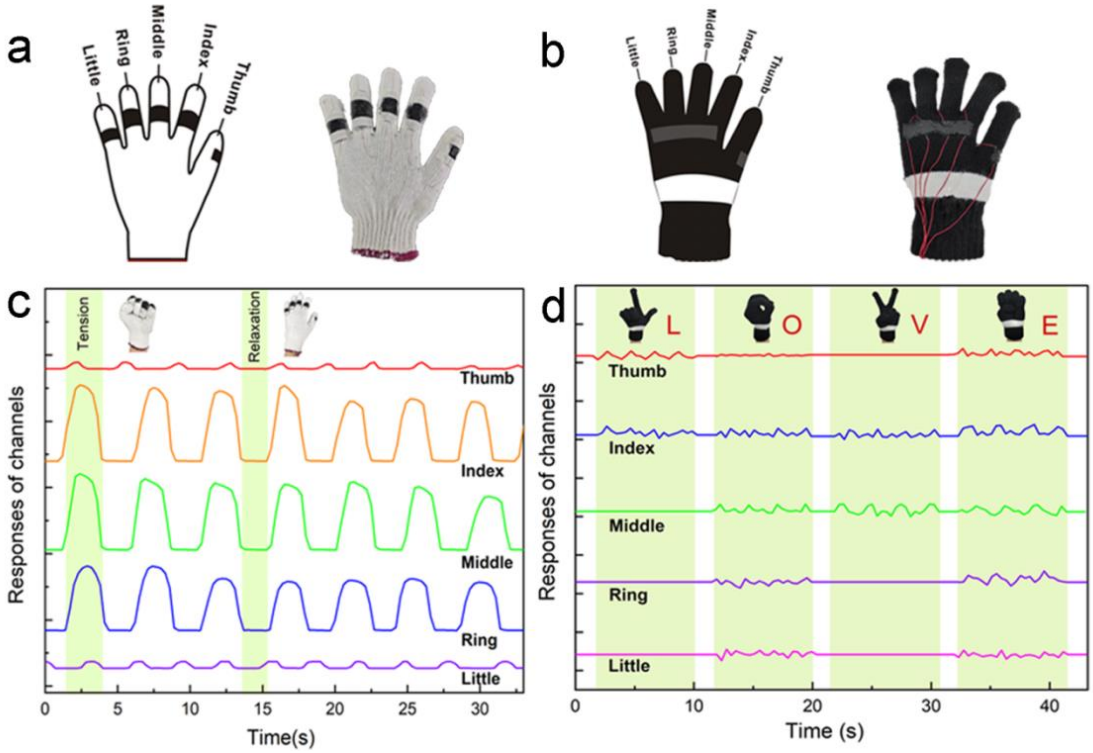

Figure 7. Illustration of PDMS-TDI-CNT nanocomposites coated on the (a) proximal interphalangeal joints of a white fabric glove and (b) metacarpophalangeal joints of a black fabric glove to detect large deformation and small deformation of finger gestures; (c) Real-

time current signals are recorded from the motion of making a fist and relaxing wearing the white glove; (d) Current signals recorded using the black glove when recognizing the international sign language of L, O, V, and E letters.

4. CONCLUSIONS

In this work, a supramolecular PDMS-based polyurethane elastomer was synthesized through a facile one-pot polycondensation reaction using aminopropyl terminated PDMS and TDI. By incorporating carboxyl-functionalized CNTs into the PDMS-TDI elastomer matrix via ultrasonication-assisted solution mixing, PDMS-TDI-CNT nanocomposite elastomers with multiple hydrogen bonds and conductive network were prepared. The successful synthesis of elastomers was verified by ^{1}H NMR and FTIR, and the uniform dispersion of CNTs in PDMS-TDI matrix was confirmed by SEM. Attributing to the high flexibility and presence of multiple hydrogen bonds, the nanocomposite elastomer showed excellent stretchability (over 1000 %) and healing efficiency (98.1 %). The strain sensor developed based on the PDMS-TDI-CNT nanocomposite possessed a high sensitivity of 2.43, fast response, and self-healing performances in the detection of various human motions including finger bending, wrist bending, elbow bending and handwriting, and different facial micro-expressions such as cheek-bulging, frowning and blinking. Thanks to the flexibility and processability of the PDMS-TDI-CNT nanocomposite, it could be easily applied to various substrates to render them with sensing capability and extend their diverse applications. A smart grip ball equipped with PDMS-TDI-CNT nanocomposite sensor units could detect the pressure applied by a patient's fingers. A sensor board based on the nanocomposite could recognize the letters written on it. Fabric gloves integrated with nanocomposite sensing units on different finger joints were able to monitor finger motion in real-time and accurately recognize the sign language. Therefore, the PDMS-TDI-CNT nanocomposite elastomer developed is promising for the development of wearable sensors for human motion detection

and intelligent devices for smart writing, gesture recognition, and human-computer interactions.

ASSOCIATED CONTENT

Supporting Information

The Supporting Information is available free of charge on the ACS Publications website.

• The GPC result of PDMS-TDI-CNT composites; comparison of self-healing performance of reported elastomers; schematic diagram of PDMS-TDI-CNT strain sensor; optical images of PDMS-TDI, PDMS-TDI/THF solution, and PDMS-TDI-CNT elastomer; thermal property of PDMS-TDI-CNT; schematic diagram of tensile direction on elastomers; self-healing property of PDMS-TDI, PDMS-TDI-4wt%CNT, and PDMS-TDI-3wt%CNT nanocomposites; mechanical properties of PDMS-TDI-CNT elastomers with different CNT concentrations; stretching process of nanocomposite elastomers; sensing performance of PDMS-TDI-CNT strain sensor (PDF).

• Movie S1, stretching process of the healed PDMS-TDI-4wt%CNT nanocomposite elastomer (MP4).

• Movie S2, real-time current changes of wrist joint bending motion of PDMS-TDI-CNT nanocomposite elastomer (MP4).

• Movie S3 and S4, real-time current signals of the smart grip ball and smart glove (MP4).

AUTHOR INFORMATION

Corredponding Author

Hao-Yang Mi – National Engineering Research Center for Advanced Polymer Processing Technology, Zhengzhou University, Zhengzhou, 450000, China; E-mail: mihaoyang@zzu.edu.cn.

Pei-Yong Feng – Key Laboratory of Advanced Packaging Materials and Technology of Hunan Province, Hunan University of Technology, Zhuzhou, 412007, China; E-mail: fpyedu@163.com.

Authors

Xin Jing – Key Laboratory of Advanced Packaging Materials and Technology of Hunan Province, Hunan University of Technology, Zhuzhou, 412007, China.

Zhenping Ma – Key Laboratory of Advanced Packaging Materials and Technology of Hunan Province, Hunan University of Technology, Zhuzhou, 412007, China.

Maxwell Fordjour Antwi-Afari – Department of Civil Engineering, College of Engineering and Physical Sciences, Aston University, Birmingham, B4 7ET, United Kingdom.

Lin Wang – National Engineering Research Center for Advanced Polymer Processing Technology, Zhengzhou University, Zhengzhou, 450000, China.

Heng Li – Department of Building and Real Estate, Hong Kong Polytechnic University, Hong Kong, 518000, China.

Yuejun Liu – Key Laboratory of Advanced Packaging Materials and Technology of Hunan Province, Hunan University of Technology, Zhuzhou, 412007, China.

Author Contributions

The manuscript was written through the contributions of all authors. All authors have given their approval to the final version of the manuscript.

Notes

The authors declare that they have no known competing financial interests or personal relationships that could have appeared to influence the work reported in this paper.

ACKNOWLEDGMENT

This work was financially supported by the Natural Research Science Foundation of Hunan Province (2020JJ4266), the Research Project of the Educational Commission of Hunan Province (18B297).

REFERENCES

1. Gu, H.; Xu, Y.; Shen, Y.; Zhu, P.; Zhao, T.; Hu, Y.; Sun, R.; Wong, C.-P., Versatile Biomass Carbon Foams for Fast Oil–Water Separation, Flexible Pressure-Strain Sensors, and Electromagnetic Interference Shielding. *Industrial & Engineering Chemistry Research* **2020,** 59, (47), 20740-20748.
2. Shi, X.; Zhang, K.; Zhao, L.; Jiang, B.; Huang, Y., Robust, Self-Healable Siloxane Elastomers Constructed by Multiple Dynamic Bonds for Stretchable Electronics and Microsystems. *Industrial & Engineering Chemistry Research* **2021,** 60, (5), 2154-2162.
3. Xu, K.; Lu, Y.; Takei, K., Multifunctional Skin-Inspired Flexible Sensor Systems for Wearable Electronics. *Advanced Materials Technologies* **2019,** 4, (3).
4. Ma, J.; Wang, P.; Chen, H.; Bao, S.; Chen, W.; Lu, H., Highly Sensitive and Large-Range Strain Sensor with a Self-Compensated Two-Order Structure for Human Motion Detection. *ACS Applied Materials & Interfaces* **2019,** 11, (8), 8527-8536.
5. Liu, H.; Zhao, H.; Li, S.; Hu, J.; Zheng, X.; Li, R.; Chen, Y.; Su, Y., Adhesion-Free Thin-Film-Like Curvature Sensors Integrated on Flexible and Wearable Electronics for Monitoring Bending of Joints and Various Body Gestures. *Advanced Materials Technologies* **2019,** 4, (2), 1800327.
6. Han, Q.; Chen, Y.; Song, W.; Zhang, M.; Wang, S.; Ren, P.; Hao, L.; Wang, A.; Bai, S.; Yin, J., Fabrication of agarose hydrogel with patterned silver nanowires for motion sensor. *Bio-Design and Manufacturing* **2019,** 2, (4), 269-277.

7. Shang, Y.; Chen, Z.; Zhang, Z.; Yang, Y.; Zhao, Y., Heart-on-chips screening based on photonic crystals. *Bio-Design and Manufacturing* **2020,** 3, (3), 266-280.
8. Zhang, C.; Zhu, P.; Lin, Y.; Tang, W.; Jiao, Z.; Yang, H.; Zou, J., Fluid-driven artificial muscles: bio-design, manufacturing, sensing, control, and applications. *Bio-Design and Manufacturing* **2021,** 4, (1), 123-145.
9. Peng, W.; Han, L.; Huang, H.; Xuan, X.; Pan, G.; Wan, L.; Lu, T.; Xu, M.; Pan, L., A direction-aware and ultrafast self-healing dual network hydrogel for a flexible electronic skin strain sensor. *Journal of Materials Chemistry A* **2020,** 8, (48), 26109-26118.
10. Zhou, Z.; Chen, K.; Li, X.; Zhang, S.; Wu, Y.; Zhou, Y.; Meng, K.; Sun, C.; He, Q.; Fan, W.; Fan, E.; Lin, Z.; Tan, X.; Deng, W.; Yang, J., Sign-to-speech translation using machine-learning-assisted stretchable sensor arrays. *Nature Electronics* **2020,** 3, 1-8.
11. Wen, N.; Zhang, L.; Jiang, D.; Wu, Z.; Li, B.; Sun, C.; Guo, Z., Emerging flexible sensors based on nanomaterials: recent status and applications. *Journal of Materials Chemistry A* **2020,** 8, (48), 25499-25527.
12. Wang, J.; Lou, H.; Meng, J.; Peng, Z.; Wang, B.; Wan, J., Stretchable energy storage E-skin supercapacitors and body movement sensors. *Sensors and Actuators B: Chemical* **2020,** 305, 127529.
13. Wang, Y.; Hao, J.; Huang, Z.; Zheng, G.; Dai, K.; Liu, C.; Shen, C., Flexible electrically resistive-type strain sensors based on reduced graphene oxide-decorated electrospun polymer fibrous mats for human motion monitoring. *Carbon* **2018,** 126, 360-371.
14. Ha, S.-H.; Ha, S.-H.; Jeon, M.-B.; Cho, J. H.; Kim, J.-M., Highly sensitive and selective multidimensional resistive strain sensors based on a stiffness-variant stretchable substrate. *Nanoscale* **2018,** 10, (11), 5105-5113.

15. Yang, Y.; Ye, Z.; Liu, X.; Su, J., A healable waterborne polyurethane synergistically cross-linked by hydrogen bonds and covalent bonds for composite conductors. *Journal of Materials Chemistry C* **2020,** 8, (15), 5280-5292.
16. Campanella, A.; Döhler, D.; Binder, W. H., Self-Healing in Supramolecular Polymers. *Macromolecular Rapid Communications* **2018,** 39, (17), 1700739.
17. Amjadi, M.; Kyung, K. U.; Park, I.; Sitti, M. J. A. F. M., Stretchable, Skin-Mountable, and Wearable Strain Sensors and Their Potential Applications: A Review. **2016,** 26, (11).
18. Gao, G.; Yang, F.; Zhou, F.; He, J.; Lu, W.; Xiao, P.; Yan, H.; Pan, C.; Chen, T.; Wang, Z. L., Bioinspired Self-Healing Human–Machine Interactive Touch Pad with Pressure-Sensitive Adhesiveness on Targeted Substrates. *Advanced Materials* **2020,** 32, (50), 2004290.
19. Zhu, Y.; Liu, J.; Guo, T.; Wang, J. J.; Tang, X.; Nicolosi, V., Multifunctional Ti3C2Tx MXene Composite Hydrogels with Strain Sensitivity toward Absorption-Dominated Electromagnetic-Interference Shielding. *ACS Nano* **2021**.
20. Das, S.; Martin, P.; Vasilyev, G.; Nandi, R.; Amdursky, N.; Zussman, E., Processable, Ion-Conducting Hydrogel for Flexible Electronic Devices with Self-Healing Capability. *Macromolecules* **2020,** 53, (24), 11130-11141.
21. Fan, J.; Huang, J.; Gong, Z.; Cao, L.; Chen, Y., Toward Robust, Tough, Self-Healable Supramolecular Elastomers for Potential Application in Flexible Substrates. *ACS Applied Materials & Interfaces* **2020**.
22. Jing, X.; Mi, H.-Y.; Lin, Y.-J.; Enriquez, E.; Peng, X.-F.; Turng, L.-S., Highly Stretchable and Biocompatible Strain Sensors Based on Mussel-Inspired Super-Adhesive Self-Healing Hydrogels for Human Motion Monitoring. *ACS Applied Materials & Interfaces* **2018,** 10, (24), 20897-20909.

23. Wang, X.; Zhan, S.; Lu, Z.; Li, J.; Yang, X.; Qiao, Y.; Men, Y.; Sun, J., Healable, Recyclable, and Mechanically Tough Polyurethane Elastomers with Exceptional Damage Tolerance. *Adv Mater* **2020**, e2005759.
24. Jing, X.; Mi, H.-Y.; Peng, X.-F.; Turng, L.-S., Biocompatible, self-healing, highly stretchable polyacrylic acid/reduced graphene oxide nanocomposite hydrogel sensors via mussel-inspired chemistry. *Carbon* **2018,** 136, 63-72.
25. Wang, X.; Zhang, H.; Yang, B.; Wang, L.; Sun, H., A colorless, transparent and self-healing polyurethane elastomer modulated by dynamic disulfide and hydrogen bonds. *New Journal of Chemistry* **2020,** 44, (15), 5746-5754.
26. Pu, W.; Fu, D.; Wang, Z.; Gan, X.; Lu, X.; Yang, L.; Xia, H., Realizing Crack Diagnosing and Self-Healing by Electricity with a Dynamic Crosslinked Flexible Polyurethane Composite. *Advanced Science* **2018,** 5, (5), 1800101.
27. Hu, J.; Mo, R.; Jiang, X.; Sheng, X.; Zhang, X., Towards mechanical robust yet self-healing polyurethane elastomers via combination of dynamic main chain and dangling quadruple hydrogen bonds. *Polymer* **2019,** 183, 121912.
28. Zhang, Q.; Niu, S.; Wang, L.; Lopez, J.; Chen, S.; Cai, Y.; Du, R.; Liu, Y.; Lai, J.; Liu, L., An Elastic Autonomous Self-Healing Capacitive Sensor Based on a Dynamic Dual Crosslinked Chemical System. *Advanced Materials* **2018,** 30, (33), 1801435.
29. Raimondo, M.; Naddeo, C.; Vertuccio, L.; Bonnaud, L.; Dubois, P.; Binder, W. H.; Sorrentino, A.; Guadagno, L., Multifunctionality of structural nanohybrids: the crucial role of carbon nanotube covalent and non-covalent functionalization in enabling high thermal, mechanical and self-healing performance. *Nanotechnology* **2020,** 31, (22), 225708.

30. Zheng, Q.; Ma, Z.; Gong, S., Multi-stimuli-responsive self-healing metallo-supramolecular polymer nanocomposites. *Journal of Materials Chemistry A* **2016,** 4, (9), 3324-3334.
31. Son, D.; Bao, Z., Nanomaterials in Skin-Inspired Electronics: Toward Soft and Robust Skin-like Electronic Nanosystems. *ACS Nano* **2018,** 12, (12), 11731-11739.
32. Liu, S.; Lin, Y.; Wei, Y.; Chen, S.; Zhu, J.; Liu, L., A high performance self-healing strain sensor with synergetic networks of poly(ε-caprolactone) microspheres, graphene and silver nanowires. *Composites Science and Technology* **2017,** 146, 110-118.
33. Guo, Q.; Zhang, X.; Zhao, F.; Song, Q.; Su, G.; Tan, Y.; Tao, Q.; Zhou, T.; Yu, Y.; Zhou, Z.; Lu, C., Protein-Inspired Self-Healable Ti3C2 MXenes/Rubber-Based Supramolecular Elastomer for Intelligent Sensing. *ACS Nano* **2020,** 14, (3), 2788-2797.
34. Ye, G.; Song, Z.; Yu, T.; Tan, Q.; Zhang, Y.; Chen, T.; He, C.; Jin, L.; Liu, N., Dynamic Ag-N Bond Enhanced Stretchable Conductor for Transparent and Self-Healing Electronic Skin. *ACS Applied Materials & Interfaces* **2020,** 12, (1), 1486-1494.
35. Feng, P.; Ji, H.; Zhang, L.; Luo, X.; Leng, X.; He, P.; Feng, H.; Zhang, J.; Ma, X.; Zhao, W., Highly stretchable patternable conductive circuits and wearable strain sensors based on polydimethylsiloxane and silver nanoparticles. *Nanotechnology* **2019,** 30, (18), 185501.
36. Wang, Z.; Lu, X.; Sun, S.; Yu, C.; Xia, H., Preparation, characterization and properties of intrinsic self-healing elastomers. *Journal of Materials Chemistry B* **2019,** 7, (32), 4876-4926.
37. Han, J.; Lu, K.; Yue, Y.; Mei, C.; Huang, C.; Wu, Q.; Xu, X., Nanocellulose-templated assembly of polyaniline in natural rubber-based hybrid elastomers toward flexible electronic conductors. *Industrial Crops and Products* **2019,** 128, 94-107.

38. Zhang, L.; Li, H.; Lai, X.; Gao, T.; Zeng, X., Three-Dimensional Binary-Conductive-Network Silver Nanowires@Thiolated Graphene Foam-Based Room-Temperature Self-Healable Strain Sensor for Human Motion Detection. *ACS Applied Materials & Interfaces* **2020,** 12, (39), 44360-44370.
39. Yang, Z.; Li, H.; Zhang, L.; Lai, X.; Zeng, X., Highly stretchable, transparent and room-temperature self-healable polydimethylsiloxane elastomer for bending sensor. *Journal of Colloid and Interface Science* **2020,** 570, 1-10.
40. Yue; Lai; Xiao; Kuang; Ping; Zhu; Miaoming; Huang; Xia; Dong, Colorless, Transparent, Robust, and Fast Scratch-Self-Healing Elastomers via a Phase-Locked Dynamic Bonds Design. *Advanced Materials* **2018**.
41. Kang, J.; Son, D.; Wang, G.-J. N.; Liu, Y.; Lopez, J.; Kim, Y.; Oh, J. Y.; Katsumata, T.; Mun, J.; Lee, Y.; Jin, L.; Tok, J. B.-H.; Bao, Z., Tough and Water-Insensitive Self-Healing Elastomer for Robust Electronic Skin. **2018,** 30, (13), 1706846.
42. Wang, P.; Yang, L.; Dai, B.; Yang, Z.; Guo, S.; Gao, G.; Xu, L.; Sun, M.; Yao, K.; Zhu, J., A self-healing transparent polydimethylsiloxane elastomer based on imine bonds. *European Polymer Journal* **2020,** 123.
43. Wu, X.; Wang, J.; Huang, J.; Yang, S., Robust, Stretchable, and Self-Healable Supramolecular Elastomers Synergistically Cross-Linked by Hydrogen Bonds and Coordination Bonds. *ACS Applied Materials & Interfaces* **2019,** 11, (7), 7387-7396.
44. Zhang, D.-D.; Ruan, Y.-B.; Zhang, B.-Q.; Qiao, X.; Deng, G.; Chen, Y.; Liu, C.-Y., A self-healing PDMS elastomer based on acylhydrazone groups and the role of hydrogen bonds. *Polymer* **2017,** 120, 189-196.
45. Zhang, X. X.; Xia, B. B.; Ye, H. P.; Zhang, Y. L.; Xiao, B.; Yan, L. H.; Lv, H. B.; Jiang, B., One-step sol–gel preparation of PDMS–silica ORMOSILs as environment-resistant

and crack-free thick antireflective coatings. *Journal of Materials Chemistry* **2012,** 22, (26), 13132-13140.

46. Kim, S. M.; Jeon, H.; Shin, S. H.; Park, S. A.; Jegal, J.; Hwang, S. Y.; Oh, D. X.; Park, J., Self-Healing Materials: Superior Toughness and Fast Self-Healing at Room Temperature Engineered by Transparent Elastomers (Adv. Mater. 1/2018). *Advanced Materials* **2018,** 30, (1), 1870001.
47. Ling, L.; Liu, F.; Li, J.; Zhang, G.; Sun, R.; Wong, C.-P., Self-Healable and Mechanically Reinforced Multidimensional-Carbon/Polyurethane Dielectric Nanocomposite Incorporates Various Functionalities for Capacitive Strain Sensor Applications. *Macromolecular Chemistry and Physics* **2018,** 219, (23), 1800369.
48. Gong, H.; Gao, Y.; Jiang, S.; Sun, F., Photocured Materials with Self-Healing Function through Ionic Interactions for Flexible Electronics. *ACS Applied Materials & Interfaces* **2018,** 10, (31), 26694-26704.
49. Wang, Z.; Lu, X.; Sun, S.; Yu, C.; Xia, H. J. J. o. M. C. B., Preparation, characterization and properties of intrinsic self-healing elastomers. *Journal of Materials Chemistry B* **2019,** 7, (32), 4876-4926.
50. Li, Y.; Yang, Z.; Ding, L.; Pan, L.; Lin, C., Feasible self-healing CL-20 based PBX: Employing a novel polyurethane-urea containing disulfide bonds as polymer binder. *Reactive and Functional Polymers* **2019,** 144, 104342.
51. Chen, Z.; Lu, H., Constructing sacrificial bonds and hidden lengths for ductile graphene/polyurethane elastomers with improved strength and toughness. *Journal of Materials Chemistry* **2012,** 22, (25), 12479-12490.
52. Yang, Z.; Wang, F.; Zhang, C.; Li, J.; Zhang, R.; Wu, Q.; Chen, T.; Sun, P., Bio-inspired self-healing polyurethanes with multiple stimulus responsiveness. *Polymer Chemistry* **2019,** 10, (24), 3362-3370.

53. Amjadi, M.; Kyung, K.-U.; Park, I.; Sitti, M., Stretchable, Skin-Mountable, and Wearable Strain Sensors and Their Potential Applications: A Review. *Advanced Functional Materials* **2016,** 26, (11), 1678-1698.

54. Wang, S.; Fang, Y.; He, H.; Zhang, L.; Li, C. a.; Ouyang, J., Wearable Stretchable Dry and Self-Adhesive Strain Sensors with Conformal Contact to Skin for High-Quality Motion Monitoring. n/a, (n/a), 2007495.

55. Park, S.; Ahn, S.; Sun, J.; Bhatia, D.; Choi, D.; Yang, K. S.; Bae, J.; Park, J.-J., Highly Bendable and Rotational Textile Structure with Prestrained Conductive Sewing Pattern for Human Joint Monitoring. *Advanced Functional Materials* **2019,** 29, (10), 1808369.

56. Wu, X.; Han, Y.; Zhang, X.; Lu, C., Highly Sensitive, Stretchable, and Wash-Durable Strain Sensor Based on Ultrathin Conductive Layer@Polyurethane Yarn for Tiny Motion Monitoring. *ACS Applied Materials & Interfaces* **2016,** 8, (15), 9936-9945.

57. Yan, C.; Wang, J.; Kang, W.; Cui, M.; Wang, X.; Foo, C. Y.; Chee, K. J.; Lee, P. S., Highly Stretchable Piezoresistive Graphene–Nanocellulose Nanopaper for Strain Sensors. *Advanced Materials* **2014,** 26, (13), 2022-2027.

58. Xuan, H.; Dai, W.; Zhu, Y.; Ren, J.; Zhang, J.; Ge, L., Self-Healing, antibacterial and sensing nanoparticle coating and its excellent optical applications. *Sensors and Actuators B: Chemical* **2018,** 257, 1110-1117.

59. Zhao, J.; Han, S.; Yang, Y.; Fu, R.; Ming, Y.; Lu, C.; Liu, H.; Gu, H.; Chen, W., Passive and Space-Discriminative Ionic Sensors Based on Durable Nanocomposite Electrodes toward Sign Language Recognition. *ACS Nano* **2017,** 11, (9), 8590-8599.

60. Guoying Gu, H. X., Sai Peng, Ling Li, Sujie Chen, Tongqing Lu, and Xiaojun Guo, Integrated Soft Ionotronic Skin with Stretchable and Transparent Hydrogel–Elastomer Ionic Sensors for Hand-Motion Monitoring. *Soft robotics* **2019,** 6, (3), 368-376.

Graphical Abstract